

Published in final edited form as:

Biomaterials. 2010 May ; 31(14): 3848–3857. doi:10.1016/j.biomaterials.2010.01.093.

Human umbilical cord stem cell encapsulation in calcium phosphate scaffolds for bone engineering

Liang Zhao^a, Michael D. Weir^a, and Hockin H.K. Xu^{a,b,c,*}

^aDepartment of Endodontics, Prosthodontics and Operative Dentistry, University of Maryland Dental School, Baltimore, MD 21201, USA

^bCenter for Stem Cell Biology and Regenerative Medicine, University of Maryland School of Medicine, Baltimore, MD 21201, USA

^cDepartment of Mechanical Engineering, University of Maryland, Baltimore County, MD 21250, USA

Abstract

Human bone marrow mesenchymal stem cells (hBMSCs) require an invasive procedure to harvest, and have lower self-renewal potential with aging. Umbilical cord mesenchymal stem cells (hUCMSCs) are a relatively new stem cell source; this study reveals a self-setting and load-bearing calcium phosphate construct that encapsulates these stem cells. The flexural strength (mean \pm sd; $n = 5$) of the hUCMSC-encapsulating calcium phosphate cement (CPC) increased from (3.5 ± 1.1) MPa without polyglactin fibers, to (11.7 ± 2.1) MPa with 20% of polyglactin fibers ($p < 0.05$). hUCMSCs attached to the bone mineral-mimicking scaffold in the osteogenic media and differentiated down the osteogenic lineage, yielding elevated alkaline phosphatase (ALP) and osteocalcin (OC) gene expressions. ALP and OC on the CPC-fiber scaffold was 2-fold those on CPC control without fibers. hUCMSCs encapsulated inside the scaffolds retained excellent viability and cell density. The encapsulated hUCMSCs inside four different constructs successfully differentiated down the osteogenic lineage and synthesized bone minerals, as confirmed by mineral staining, SEM, and XRD. The percentage of mineral area synthesized by the encapsulated hUCMSCs increased from about 3% at day-7, to 12% at day-21 ($p < 0.05$). In conclusion, this study demonstrated that hUCMSCs encapsulated in the bioengineered scaffolds osteo-differentiated and synthesized bone minerals. The self-setting CPC-chitosan-fiber scaffold supported the viability and osteogenic differentiation of the encapsulated hUCMSCs, and had mechanical strength matching that of cancellous bone.

Keywords

Umbilical cord stem cells; Calcium phosphate cement scaffolds; Cell encapsulation; Osteogenic differentiation; Load-bearing; Bone tissue engineering

1. Introduction

Stem cell-based tissue engineering has the potential to revolutionize medicine with the ability to regenerate damaged and diseased tissues [1-5]. Bone defects can arise from trauma, disease, congenital deformity and tumor resection. Bone fracture occurs to nearly seven million people each year in the United States, and musculoskeletal conditions cost \$215 billion annually [6,

© 2010 Elsevier Ltd. All rights reserved.

*Corresponding author. Department of Endodontics, Prosthodontics and Operative Dentistry, University of Maryland Dental School, Center for Stem Cell Biology and Regenerative Medicine, Baltimore, MD 21201, USA. Tel.: +1 410 706 7047; fax: +1 410 706 3028. hxu@umaryland.edu (H.H.K. Xu).

7]. In bone engineering, a scaffold can be used to deliver cells guided for osteogenesis [8-10]. Human bone marrow mesenchymal stem cells (hBMSCs) can differentiate into osteoblasts, adipocytes, chondrocytes, myoblasts, neurons and fibroblasts [9]. hBMSCs can be harvested from the patient, expanded in culture, induced to differentiate and combined with a scaffold to repair bone defects. There is enormous economic importance to these new approaches [7,9].

However, autogenous hBMSCs require an invasive procedure, are limited in number, and have lower self-renewal potential with aging. Recently, human umbilical cord mesenchymal stem cells (hUCMSCs) were differentiated into adipocytes, osteoblasts, chondrocytes, neurons, and other cells [11-16]. hUCMSCs are advantageous because umbilical cords can be collected at a low cost to be an inexhaustible stem cell source. Their harvest does not require the invasive procedure of hBMSCs, and does not have the controversies of human embryonic stem cells (hESCs). Furthermore, hUCMSCs are primitive MSCs and exhibit a high plasticity and developmental flexibility [12]. In addition, hUCMSCs appear to cause no immunorejection *in vivo* [12]. In recent studies, hUCMSCs were cultured on the surfaces of tissue culture plastic [13], polymer scaffold [16] and calcium phosphate scaffold [17]. However, a literature search revealed no publication on hUCMSC encapsulation inside scaffolds for bone tissue engineering.

Currently, pre-formed carriers for cell delivery have drawbacks including the difficulty in seeding cells deep in the scaffold, and inability for injection in minimally invasive surgeries [7]. Current injectable carriers are weak and cannot be used in a wide range of load-bearing repairs [10,18]. For example, it was concluded that “Hydrogel scaffolds...do not possess the mechanical strength to be used in load-bearing applications” [18]. To date, an injectable, bioactive, and strong scaffold for stem cell encapsulation is yet to be developed. Calcium phosphate scaffolds are bioactive because they mimic the bone minerals and can bond to bone [19-22]. The calcium phosphate minerals provide a preferred substrate for cell attachment and expression of osteoblast phenotype [23,24]. However, for pre-formed calcium phosphate bioceramic scaffolds to fit in a bone cavity, the surgeon needs to machine the graft or carve the surgical site, leading to increases in bone loss, trauma, and surgical time [7]. In contrast, calcium phosphate cement (CPC) can be injected or molded, and set *in situ* to form a bioactive scaffold that bonds to bone [25-27]. The first CPC was approved by the Food and Drug Administration (FDA) in 1996 for craniofacial repairs [28-30]. However, due to its low strength, CPC was “limited to the reconstruction of non-stress-bearing bone” [29,30]. A literature search revealed no report on stem cell encapsulation in CPC. Our recent study [17] investigated the fatigue of CPC and hUCMSC seeding on the surface of scaffolds showing excellent proliferation; it did not investigate hUCMSC encapsulation inside the scaffold nor osteogenic differentiation.

Therefore, the objectives of this study were to encapsulate hUCMSCs in CPC composite scaffolds, to improve the strength of hUCMSC-encapsulated CPC constructs, and to examine the osteogenic differentiation of the encapsulated hUCMSCs. It was hypothesized that: (1) hUCMSCs attaching to CPC scaffolds will osteo-differentiate, yielding high levels of alkaline phosphatase activity and osteocalcin gene expressions; (2) when hUCMSCs are encapsulated inside CPC, the construct can be strengthened via absorbable fibers; and (3) hUCMSCs encapsulated inside the CPC scaffolds will osteo-differentiate and successfully synthesize bone minerals.

2. Materials and methods

2.1. Reinforcing CPC scaffold with chitosan and fibers

Calcium phosphate cement (CPC) consisted of a mixture of tetracalcium phosphate [TTCP: $\text{Ca}_4(\text{PO}_4)_2\text{O}$] and dicalcium phosphate anhydrous (DCPA: CaHPO_4) [30,31]. TTCP was

synthesized from a solid-state reaction between DCPA and CaCO_3 , and then ground in a blender to obtain particle sizes of 1–80 μm , with a median size of 17 μm . The DCPA powder was ground to obtain particle sizes of 0.4–3.0 μm , with a median of 1.0 μm . The TTCP and DCPA powders were mixed at a molar ratio of 1:1 to form the CPC powder.

Chitosan and its derivatives are natural biopolymers that are biodegradable and osteoconductive [32]. Chitosan facilitated the setting of CPC [31]. Chitosan lactate (referred to as chitosan; Vanson, Redmond, WA) was mixed with water at a chitosan/(chitosan + water) mass fraction of 15% to form the CPC liquid [33]. An absorbable fiber (Vicryl suture, polyglactin 910, Ethicon, Somerville, NJ) was used because it possessed a relatively high strength [34]. It reinforced CPC for four weeks, and then dissolved and created long macropores in CPC. The fiber was cut to a length of 8 mm for use in CPC [34]. The CPC powder was mixed with the chitosan liquid at a powder:liquid mass ratio of 3:1. The following fiber volume fractions (=fiber volume/specimen volume) were tested: 0%, 5%, 10%, 15%, and 20%. Fiber fractions $\geq 25\%$ were not tested, so that the paste was readily mixed and not dry. CPC control was also made, with 0% chitosan and 0% fibers. The specimen was set in a humidifier for 4 h at 37 °C. The hardened specimen was immersed in a physiological solution for 1 day prior to testing.

2.2. Mechanical testing

A three-point flexural test was used to fracture specimens with $3 \times 4 \times 25$ mm dimensions on a computer-controlled Universal Testing Machine (5500R, MTS, Cary, NC) [35]. The CPC-based specimens contained 50% by volume of alginate hydrogel beads encapsulating hUCMSCs as described in Section 2.5, with chitosan and fiber reinforcement as described in Section 2.1. The specimens were incubated in culture media for 1 day prior to testing. Flexural strength $S = 3F_{\text{max}}L/(2bh^2)$, where F_{max} is the maximum load on the load–displacement (F – d) curve, L is span, b is specimen width, and h is thickness. Elastic modulus $E = (F/d) (L^3/[4bh^3])$, where load F divided by displacement d is the slope. Work-of-fracture (toughness), WOF, was calculated as the area under the F – d curve divided by the specimen's cross-sectional area [34].

2.3. hUCMSC harvest and culture

hUCMSCs were generously provided by Dr. M. S. Detamore (University of Kansas, Lawrence, KS). hUCMSCs were harvested as described previously [11,16]. Briefly, umbilical cords were obtained from an obstetrician and incubated in a collagenase type I solution containing collagenase type I (300 U/mL) (Sigma, St. Louis, MO), hyaluronidase (1 mg/mL) (MP Biomedical, Aurora, OH) and calcium chloride (3 mM) (Fisher, Pittsburgh, PA), for 30 min at 37 °C. Then, the vascular tissue was removed, and the cords were minced and plated in a modified Dulbecco's modified Eagle's medium (DMEM) for 1 week as described previously [14]. The cord remnants were then removed and the attached cells were harvested. The use of hUCMSCs was approved by the University of Maryland. Cells were cultured in a low-glucose DMEM with 10% fetal bovine serum (FBS) and 1% penicillin/streptomycin (PS) (Invitrogen, Carlsbad, CA) (control media). At 80–90% confluence, hUCMSCs were detached by trypsin (Invitrogen) and passaged. Passage 4 hUCMSCs were used for experiments. The osteogenic media had 100 nM dexamethasone, 10 mM β -glycerophosphate, 0.05 mM ascorbic acid, and 10 nM $1\alpha,25$ -dihydroxyvitamin (Sigma) [13,16].

2.4. qRT-PCR measurement of hUCMSCs on CPC

hUCMSCs were seeded on the surfaces of three materials: CPC control, CPC–chitosan, and CPC–chitosan–fiber scaffold (with 20% fibers). CPC control was referred to as the FDA-approved CPC, because that material consisted of the same TTCP–DCPA mixture with no chitosan or fibers [30]. 150,000 cells [36] were diluted into 2 mL of osteogenic media and

added to each well containing a CPC disk of 2 mm thickness and 12 mm in diameter. For quantitative real-time reverse transcription polymerase chain reaction (qRT-PCR, 7900HT, Applied Biosystems, Foster City, CA), the culture was incubated for 1, 4, and 8 days [36]. The total cellular RNA on the scaffolds were extracted with TRIzol reagent (Invitrogen) and reverse-transcribed into cDNA using a High-Capacity cDNA Archive kit. TaqMan gene expression assay kits, including two pre-designed specific primers and probes, were used to measure the transcript levels of the proposed genes on human alkaline phosphatase (ALP, Hs00758162_m1), Osteocalcin (OC, Hs00609452_g1), and glyceraldehyde 3-phosphate dehydrogenase (GAPDH, Hs99999905). Relative expression level for each target gene was evaluated using the $2^{-\Delta\Delta Ct}$ method [36]. The Ct values of target genes were normalized by the Ct values of the TaqMan human housekeeping gene GAPDH to obtain the ΔCt values. These values were then subtracted by the Ct value of the hUCMSCs cultured on tissue culture polystyrene in the control media for 1 day (the calibrator) to obtain the $\Delta\Delta Ct$ values. The fold of change was obtained with $n = 5$.

2.5. hUCMSC encapsulation

The CPC paste could be injected and set to form a porous scaffold [37,38]; however, the paste mixing and setting reaction would harm the cells. Hence, hUCMSCs were encapsulated in alginate hydrogel beads, and the beads were then mixed into CPC. After CPC setting, the hydrogel beads could dissolve and release the cells, while concomitantly creating a macroporous scaffold. In this study, the hydrogel beads were not dissolved in order to facilitate cell harvest, microscopy examination and analysis. A 1.2 wt% sodium alginate solution was prepared by dissolved alginate (ProNova, Oslo, Norway) in saline. hUCMSCs were encapsulated at the density of 1,000,000 cells/mL of alginate solution. Beads were formed by extruding the cell-alginate droplets into a calcium chloride solution to gel.

Four types of constructs were fabricated: (1) hUCMSCs in alginate hydrogel beads; (2) hUCMSCs in beads in CPC; (3) hUCMSCs in beads in CPC–chitosan; (4) hUCMSCs in beads in CPC–chitosan–fiber scaffold. Construct 1 was a pile of beads, not a solid scaffold, and not load-bearing. Constructs 2–4 were able to self-set to form a hardened scaffold, and the load-bearing capability was increased with chitosan and fiber reinforcement. The first goal here was for the cells in the self-setting and injectable CPC-based constructs (#2–4) to match the cell viability and differentiation in construct 1, the hydrogel, which is known to be highly biocompatible but not load-bearing. The second goal was for the cells in construct 4 to match the cell viability and differentiation in construct 2, with the FDA-approved CPC control as its matrix. This would show that incorporating chitosan and fibers, which greatly improved the load-bearing capability of CPC, did not compromise the encapsulated hUCMSCs. For constructs 2–4, the hUCMSC-hydrogel beads and the CPC-based paste were placed into a cell culture well with the beads being completely covered by the paste, at a volume fraction of beads/(paste + beads) = 50%. Each construct was set at 37 °C for 30 min. Then, 2 mL of the osteogenic media was added to each well. At 1, 7, 14 and 21 days, the constructs were carefully broken and the cell-encapsulating beads were harvested. Cells were live/dead stained (Invitrogen). The percentage of live cells was: $P_{\text{Live}} = N_{\text{Live}} / (N_{\text{Live}} + N_{\text{Dead}})$, where N_{Live} = number of live cells, and N_{Dead} = number of dead cells [39]. In addition, the live cell density, D , was calculated: $D = N_{\text{Live}} / A$, where A is the area of the view field of the specimen on which N_{Live} was measured.

2.6. ALP, DNA, and mineral staining of encapsulated hUCMSCs

The cell-encapsulating hydrogel beads harvested as described above were dissolved by 55 mmol/L sodium citrate tribasic solution (Sigma). A colorimetric *p*-nitrophenyl phosphate (pNPP) assay (Stanbio, Boerne TX) was used to measure the ALP activity. Normal control serum containing a known concentration of ALP was used as a standard. A microplate reader

(M5 SpectraMax, Molecular Devices, Sunnyvale, CA) was used and the ALP was normalized by the DNA content [39]. DNA was quantified using the Quant-iT PicoGreen Kit (Invitrogen, Carlsbad, CA) following standard protocols.

Minerals emit red fluorescence when stained with xylenol orange (Sigma). The minerals synthesized by the stem cells in the hydrogel beads were stained and examined using both phase contrast and fluorescence images. The mineral area percentage was calculated as $A_{\text{Mineral}}/A_{\text{Total}}$, where A_{Mineral} is the area of mineralization (red fluorescence), and A_{Total} is the total area of the field of view of the image. Four images for each specimen, with five specimens at each time point for each construct, yielded twenty images for each condition.

2.7. SEM, XRD, and statistics

A scanning electron microscope (SEM, JEOL 5300, Peabody, MA) was used. hUCMSC samples were fixed with 1% glutaraldehyde, subjected to graded alcohol dehydrations, and rinsed with hexamethyldisilazane, and examined in SEM [33]. SEM and XRD were also used to examine the hUCMSC-synthesized minerals. The hydrogel beads were dried, and the resulting substance was collected. The hydrogel contained 1.2% sodium alginate and 98.8% aqueous solution. Therefore, after the beads were dried, there was little material left (at 7 days), except the substance synthesized by the cells (at 21 days). The minerals synthesized by the cells were examined using x-ray diffraction (XRD) (Rigaku, Danvers, MA) with graphite monochromatized copper K_{α} radiation. One-way and two-way ANOVA were performed to detect significant effects of the variables. Tukey's multiple comparison tests were used at a p value of 0.05.

3. Results

Fig. 1A shows a typical SEM of hUCMSCs (referred to as "C") attaching to a CPC–chitosan–fiber scaffold. Cells developed cytoplasmic extensions "E". Fig. 1B shows the cell extensions attaching to the nano-sized apatite crystals that make up the CPC matrix. In addition, live/dead staining and examination revealed numerous live cells on these specimens, with few dead cells. The qRT-PCR results (mean \pm sd; $n = 5$) are plotted in Fig. 1C and D. In each plot, bars with dissimilar letters indicate values that are significantly different ($p < 0.05$). ALP gene expression was minimal at day 1; it peaked at day 4, and then slightly decreased at day 8. OC expression peaked at day 8. Incorporating chitosan and fibers into CPC did not adversely affect the ALP and OC gene expression of hUCMSCs. Instead, the ALP and OC on the CPC–chitosan–fiber scaffold was higher than those on the FDA-approved CPC control ($p < 0.05$).

Next, hUCMSCs were encapsulated into the CPC paste, and the effects of fiber volume fraction on the load-bearing properties of the cell-CPC construct were determined. In Fig. 2, S increased from (3.5 ± 1.1) MPa for CPC–chitosan without fibers, to (11.7 ± 2.1) MPa with 20% fibers ($p < 0.05$). E increased from (0.7 ± 0.2) GPa for CPC–chitosan without fibers, to (2.0 ± 0.4) GPa with 20% fibers. WOF increased from (0.02 ± 0.01) kJ/m² for CPC–chitosan without fibers, to (1.65 ± 0.66) kJ/m² with 20% fibers. 20% CPC control containing 50% hydrogel beads had S of (2.3 ± 0.9) MPa, E of (0.5 ± 0.2) GPa, and WOF of (0.009 ± 0.005) kJ/m². The CPC–chitosan scaffold with 20% fibers, hereinafter referred to as "CPC–chitosan–fiber", had S , E and WOF that were 5-fold, 4-fold, and 183-fold, those of CPC control, respectively.

The percentage of encapsulated live cells, P_{Live} , is plotted in Fig. 3A. In general, encapsulating the hUCMSCs from 1 to 21 days had little effect on P_{Live} . P_{Live} for CPC–chitosan–fiber scaffold matched the P_{Live} for the FDA-approved CPC control ($p > 0.1$). They all matched that of the hydrogel without CPC ($p > 0.1$). The live cell density in Fig. 3B showed that: (1) encapsulation in CPC did not adversely affect the hUCMSC density, compared to those in

hydrogel without CPC; (2) the stronger CPC–chitosan–fiber scaffold did not compromise the encapsulated live cell density, compared to the FDA-approved CPC control ($p > 0.1$).

In Fig. 4A, hUCMSCs encapsulated in hydrogel or CPC pastes had similar DNA masses ($p > 0.1$). Culturing hUCMSCs in control media or in osteogenic media did not affect the DNA amount either. However, ALP was dramatically increased in the osteogenic media (Fig. 4B). ALP at day 7 was much higher in osteogenic media than those in control media. ALP peaked at day 14, and slightly decreased at day 21 ($p < 0.05$). hUCMSCs encapsulated in CPC–chitosan–fiber had ALP that matched those of the FDA-approved CPC and hydrogel controls ($p > 0.1$).

Fig. 5 shows photos of the staining of minerals synthesized by the encapsulated hUCMSCs. Little mineral was seen at 7 days, similar in all four constructs. The mineral staining amount increased at 14 days and 21 days. The mineral staining area was plotted in Fig. 6A. For each construct, the amount of hUCMSC-synthesized minerals increased with time ($p < 0.05$). Comparison between different constructs showed that: (1) encapsulation in CPC did not adversely affect the hUCMSC's synthesis of minerals compared to that in hydrogel without CPC; (2) chitosan and polyglactin fibers did not compromise the hUCMSC's ability to synthesize minerals compared to the FDA-approved CPC control.

Fig. 6B shows the substance synthesized by the encapsulated hUCMSCs, which had the morphology of mineral particles < 500 nm in size. Fig. 6C shows the XRD pattern of this substance, while Fig. 6D shows the XRD of a known hydroxyapatite (HA). The peak is lower for the hUCMSC-synthesized minerals, indicating that it is a low-crystalline apatite, consistent with the observed low crystallinity of biological minerals [19]. Ceramic HA has three strongest peaks at 31.77° , 32.19° and 32.90° [40]. For low-crystalline apatite, often just one broad peak is seen around the three strongest peaks, because they are so close together. This is consistent with the one peak in Fig. 6C and D. The peaks in the same vicinity of 32° in Fig. 6C and D indicate that the substance synthesized by the hUCMSCs was apatitic.

4. Discussion

hUCMSCs are promising as an inexhaustible and low-cost alternative to the gold-standard hBMSCs which require an invasive procedure to harvest. In previous studies, hUCMSCs were successfully guided for osteo-differentiation on two-dimensional tissue culture plastics [11-13]. Two meritorious studies have seeded pre-formed polyglycolic acid scaffolds with hUCMSCs for cartilage and osteogenic differentiation [14,16]. In another study [41], human cord blood-derived mesenchymal stem cells were seeded onto a collagen/tricalcium phosphate scaffold and showed significant engraftment in rat femoral defects. Literature search revealed no publication on hUCMSC encapsulation in injectable and load-bearing scaffolds for bone tissue engineering. In the present study, hUCMSCs were encapsulated in alginate hydrogel, in CPC, in CPC–chitosan scaffold, and in CPC–chitosan–fiber scaffold. The ultimate aim of this study was the encapsulation of stem cells in the injectable CPC-based scaffold for *in vivo* applications. hUCMSCs survived the CPC paste mixing and cement setting reaction. The encapsulated hUCMSCs in the scaffolds had excellent viability, and maintained the percentage of live cells and cell density after three weeks of encapsulation. The encapsulated hUCMSCs successfully differentiated down the osteogenic lineage. ALP showed a 20-fold increase at 14 days, compared to that in control media (Fig. 4B). ALP is an enzyme expressed by MSCs during osteogenesis and is a well-defined marker for their differentiation [42-45]. A previous study showed that MSCs grown on a bioactive glass had higher ALP than that on tissue culture plastic [45]. Another study used silk scaffolds for bone engineering and showed that the ALP of hMSCs cultured in the osteogenic medium was approximately 3-fold the ALP for cells cultured in the control medium [43].

The present study showed that the ALP gene expression peaked at 4-day, while the ALP via the pNPP assay peaked at 14-day. This is because at an early stage of differentiation, the genetic expression of ALP is upregulated. This sets off a cascade of events which lead to the production of the ALP enzyme. The RT-PCR method measures the gene expression of ALP. The genetic regulation precedes the protein production, hence the gene expression of markers occurs at an earlier time. On the other hand, the pNPP assay measures the activity of the ALP enzyme secreted by the cells during differentiation, which occurs at a later time. Our results are consistent with previous reports. For example, a previous study showed that the expression of ALP measured via RT-PCR was minimal at 1 day; it peaked at 4 days, and then decreased at 8 days [36]. That study also observed that the osteocalcin expression peaked at 8 days, slightly later than the ALP peak [36]. These results are consistent with Fig. 1C and D of the present study. Other studies using the pNPP assay showed that hMSCs in a hydrogel differentiated and had a 14-day ALP peak that was 1.5–2.5 times the ALP at 1 day [42]. Another study showed that the ALP activity peaked at 2 weeks which was two-fold the ALP at 1 day [44]. These studies are consistent with the ALP peaking at 14 days as measured by the pNPP assay (Fig. 4).

Furthermore, the present study showed that ALP and osteocalcin gene expressions were higher when the hUCMSCs were seeded on CPC–chitosan–fiber scaffold, than on the CPC without fibers (Fig. 1C and D). The polyglactin fiber used in CPC consisted of individual fibers about 14 μm in diameter, that were braided to form a bundle having a diameter of about 300 μm with a rough surface [34]. The surfaces of the CPC–chitosan–fiber specimens were noticeably rougher than the CPC specimens without fibers. It is possible that the rougher surface of the CPC–chitosan–fiber scaffold facilitated the cell attachment and osteogenic differentiation. For example, a recent study showed a dramatic, 3-fold greater bone tissue ingrowth in defects containing carbon-nanotube nanocomposite scaffold, compared to control polymer scaffolds without nanotubes [46]. This increase was related to the high surface area and roughness that may have enhanced cell attachment and stimulated the cells to synthesize the extracellular matrix [46]. Further study is needed to investigate whether the novel CPC–chitosan–fiber scaffold would be advantageous for bone regeneration *in vivo* compared to CPC without fibers.

When the culture was prolonged to 21 days, the hUCMSCs successfully synthesized bone minerals while being encapsulated in hydrogel, in CPC, in CPC–chitosan, and in CPC–chitosan–fiber scaffolds. Literature search revealed that this is the first report on hUCMSC encapsulation inside constructs with successful synthesis of bone minerals. The amount of mineralization increased with time (Fig. 6A). SEM and XRD confirmed that the cell-synthesized mineral was apatitic. These results demonstrated that: (i) hUCMSCs encapsulated in a novel self-setting CPC–chitosan–fiber scaffold can osteo-differentiate and synthesize bone minerals; (ii) encapsulation in CPC does not adversely affect the hUCMSCs' ability to synthesize minerals compared to those in hydrogel without CPC; (iii) adding chitosan and fibers, which greatly improved the load-bearing capability, did not compromise the mineral synthesis by the encapsulated hUCMSCs, compared to the FDA-approved CPC control.

Injectable constructs are highly desirable because they can be injected and molded, and then harden *in situ* [10,26,37,38]. Previous injectable carriers are mechanically weak [18,47–49]. The present study developed the first injectable, load-bearing and stem cell-encapsulating CPC construct. CPC pastes could be injected through a 10-gauge needle even when the paste contained porogen and chopped fibers [37,38]. The constructs in the present study contained hydrogel beads, chitosan and fibers which may require a larger injection force; further study is needed to examine the paste injectability and the cell viability after injection. The injectable system has the potential to shorten the surgical time, avoid the damage of large muscle retraction, reduce postoperative pain and scar size, facilitate rapid recovery and reduce cost. Previous studies have developed other types of meritorious injectable carriers. For example,

an injectable polymeric carriers for cell delivery had a strength of 0.7 MPa [47]. Hydrogels for cell delivery had a strength of about 0.1 MPa [48,49]. While these systems are useful for non-load-bearing applications, their strengths are much lower than the natural cancellous bone's tensile strength of 3.5 MPa [50]. In contrast, the novel CPC–chitosan–fiber construct containing hUCMSCs had a flexural strength exceeding 10 MPa, which matched/exceeded the reported strength of cancellous bone. This strength is more than 10-fold higher than those of previous injectable carriers for cell delivery [47-49].

The hUCMSC-encapsulating CPC–chitosan–fiber construct had a modulus of 0.9 GPa, exceeding the 0.3 GPa for cancellous bone [51]. Both are much higher than the 0.008 GPa for an injectable polymeric carrier [47], and 0.0001 GPa for hydrogels [48,49]. Therefore, the novel CPC–chitosan–fiber/hUCMSC construct is much stronger than previous injectable carriers for cell delivery, and may find utility in a wide range of orthopedic applications. The fibers in CPC would start to degrade after about four weeks which would weaken the construct. However, previous studies have shown that it was in the early stage of implantation when strength was most needed, because the strength of macroporous implants increased over time once new bone started to grow in the macropores [52]. Hence, the rationale for using the fibers was to provide the needed early-strength. It was hoped that after about four weeks *in vivo*, significant new bone formation would have occurred, which would increase the implant strength to compensate for the weakening from fiber degradation. *In vivo* studies are needed to investigate the construct strength and elastic modulus versus time. In addition, the present study showed that the cells in the hydrogel were viable and able to osteo-differentiate, but were not proliferating, consistent with previous studies [53]. It would be desirable to have the hydrogel to rapidly degrade after CPC setting, and release the cells to attach to the CPC matrix. CPC was shown to support cell proliferation [17,39]. Therefore, further study is needed to facilitate hydrogel bead degradation and cell proliferation inside CPC-based scaffolds for bone tissue engineering.

Potential applications for this self-setting, load-bearing and hUCMSC-encapsulating CPC construct include the major reconstructions of the maxilla and mandible, and other craniofacial restorations. These repairs could benefit from a highly biocompatible and osteoconductive CPC scaffold that can be molded to the desired shape for esthetics, with improved fracture resistance and stem cell encapsulation for rapid osteogenesis. Other orthopedic repairs include bone regeneration after trauma or tumor resection, *in situ* fracture fixation, and percutaneous vertebroplasty to fill and strengthen osteoporotic bone lesions at risk for fracture. Further *in vivo* studies are needed to realize such potentials.

5. Conclusions

In the present study, novel stem cell-encapsulated, self-setting and stress-bearing CPC composite constructs were developed for bone tissue engineering. The hUCMSC-encapsulating CPC–chitosan–fiber construct exceeded the strength of cancellous bone. hUCMSCs encapsulated in the self-setting, bioactive scaffolds showed excellent viability, successfully osteo-differentiated, and synthesized bone minerals. These results support the use of hUCMSCs as an inexhaustible, low-cost and potent alternative to the gold-standard hBMSCs, which require an invasive procedure to harvest. Hence, these results may broadly impact the field of stem cell-based regenerative medicine. The self-setting, mechanically-strong, and stem cell-encapsulating CPC composite scaffold may find utility in a wide range of craniofacial and orthopedic repairs, with the potential to greatly enhance bone regeneration. Further animal studies are needed to investigate the stem cell-encapsulated, self-setting and stress-bearing CPC composite constructs.

Acknowledgments

We are indebted to Prof. M. S. Detamore at the University of Kansas, Lawrence, KS for kindly providing the human umbilical cord stem cells. We thank Drs. L. C. Chow, S. Takagi and A. A. Giuseppetti at the Paffenbarger Research Center, Dr. Carl G. Simon at the National Institute of Standards and Technology, and Dr. John Fisher at the University of Maryland for discussions and help. This study was supported by NIH R01 grants DE14190 and DE17974 (HX), Maryland Stem Cell Research Fund (HX), and the University of Maryland Dental School.

Appendix

Figures with essential colour discrimination. Certain figures in this article, in particular Figs. 1-6, are difficult to interpret in black and white. The full colour images can be found in the on-line version, at doi:10.1016/j.biomaterials.2010.01.093

References

- [1]. Sikavitsas VI, Bancroft GN, Holtorf HL, Jansen JA, Mikos AG. Mineralized matrix deposition by marrow stromal osteoblasts in 3D perfusion culture increases with increasing fluid shear forces. *Proc Natl Acad Sci USA* 2003;100:14683–8. [PubMed: 14657343]
- [2]. Mauney J, Volloch V, Kaplan DL. Matrix-mediated retention of osteogenic differentiation potential by human adult bone marrow stromal cells during ex vivo expansion. *Biomaterials* 2004;25:3233–43. [PubMed: 14980418]
- [3]. Yao J, Radin S, Reilly G, Leboy PS, Ducheyne P. Solution-mediated effect of bioactive glass in poly (lactic-co-glycolic acid)-bioactive glass composites on osteogenesis of marrow stromal cells. *J Biomed Mater Res* 2005;75A:794–801.
- [4]. Mao JJ, Giannobile WV, Helms JA, Hollister SJ, Krebsbach PH, Longaker MT, et al. Craniofacial tissue engineering by stem cells. *J Dent Res* 2006;85:966–79. [PubMed: 17062735]
- [5]. Datta N, Pham QP, Sharma U, Sikavitsas VI, Jansen JA, Mikos AG. *In vitro* generated extracellular matrix and fluid shear stress synergistically enhance 3D osteoblastic differentiation. *Proc Natl Acad Sci USA* 2006;103:2488–93. [PubMed: 16477044]
- [6]. Praemer, A.; Furner, S.; Rice, DP. Musculoskeletal conditions in the United States. American Academy of Orthopaedic Surgeons; Rosemont, Illinois: 1999. chapter 1
- [7]. Laurencin CT, Ambrosio AMA, Borden MD, Cooper JA. Tissue engineering: orthopedic applications. *Annual Rev Biomed Eng* 1999;1:19–46. [PubMed: 11701481]
- [8]. Silva GA, Coutinho OP, Ducheyne P, Reis RL. Materials in particulate form for tissue engineering, part 2: applications in bone (review). *J Tissue Eng Regen Med* 2007;1:97–109. [PubMed: 18038398]
- [9]. Mao, JJ.; Vunjak-Novakovic, G.; Mikos, AG.; Atala, A. Regenerative medicine: translational approaches and tissue engineering. Artech House; Boston and London: 2007.
- [10]. Kretlow JD, Young S, Klouda L, Wong M, Mikos AG. Injectable biomaterials for regenerating complex craniofacial tissues. *Adv Mater* 2009;21:3368–93. [PubMed: 19750143]
- [11]. Wang HS, Hung SC, Peng ST. Mesenchymal stem cells in the Wharton's jelly of the human umbilical cord. *Stem Cells* 2004;22:1330–7. [PubMed: 15579650]
- [12]. Can A, Karahuseyinoglu S. Concise review: human umbilical cord stroma with regard to the source of fetus-derived stem cells. *Stem Cells* 2007;25:2886–95. [PubMed: 17690177]
- [13]. Baksh D, Yao R, Tuan RS. Comparison of proliferative and multilineage differentiation potential of human mesenchymal stem cells derived from umbilical cord and bone marrow. *Stem Cells* 2007;25:1384–92. [PubMed: 17332507]
- [14]. Bailey MM, Wang L, Bode CJ, Mitchell KE, Detamore MS. A comparison of human umbilical cord matrix stem cells and temporomandibular joint condylar chondrocytes for tissue engineering temporomandibular joint condylar cartilage. *Tissue Eng* 2007;13:2003–10. [PubMed: 17518722]
- [15]. Karahuseyinoglu S, Kocaepe C, Balci D, Erdemli E, Can A. Functional structure of adipocytes differentiated from human umbilical cord stroma-derived stem cells. *Stem Cells* 2008;26:682–91. [PubMed: 18192234]

- [16]. Wang L, Singh M, Bonewald LF, Detamore MS. Signaling strategies for osteogenic differentiation of human umbilical cord mesenchymal stromal cells for 3D bone tissue engineering. *J Tissue Eng Regen Med* 2009;3:398–404. [PubMed: 19434662]
- [17]. Zhao R, Burguera EF, Xu HHK, Amin N, Ryou H, Arola DD. Fatigue and human umbilical cord stem cell seeding characteristics of calcium phosphate-chitosan-biodegradable fiber scaffolds. *Biomaterials* 2010;31:840–7. [PubMed: 19850337]
- [18]. Drury JL, Mooney DJ. Review. Hydrogels for tissue engineering: scaffold design variables and applications. *Biomaterials* 2003;24:4337–51. [PubMed: 12922147]
- [19]. LeGeros RZ. Biodegradation and bioresorption of calcium phosphate ceramics. *Clin Mater* 1993;14:65–88. [PubMed: 10171998]
- [20]. Ducheyne P, Qiu Q. Bioactive ceramics: the effect of surface reactivity on bone formation and bone cell function. *Biomaterials* 1999;20:2287–303. [PubMed: 10614935]
- [21]. Pilliar RM, Filiaggi MJ, Wells JD, Grynblas MD, Kandel RA. Porous calcium polyphosphate scaffolds for bone substitute applications – in vitro characterization. *Biomaterials* 2001;22:963–72. [PubMed: 11311015]
- [22]. Foppiano S, Marshall SJ, Marshall GW, Saiz E, Tomsia AP. The influence of novel bioactive glasses on in vitro osteoblast behavior. *J Biomed Mater Res A* 2004;71:242–9. [PubMed: 15372470]
- [23]. Radin S, Reilly G, Bhargava G, Leboy PS, Ducheyne P. Osteogenic effects of bioactive glass on bone marrow stromal cells. *J Biomed Mater Res A* 2005;73:21–9. [PubMed: 15693019]
- [24]. Deville S, Saiz E, Nalla RK, Tomsia AP. Freezing as a path to build complex composites. *Science* 2006;311:515–8. [PubMed: 16439659]
- [25]. Barralet JE, Gaunt T, Wright AJ, Gibson IR, Knowles JC. Effect of porosity reduction by compaction on compressive strength and microstructure of calcium phosphate cement. *J Biomed Mater Res B* 2002;63:1–9.
- [26]. Bohner M, Baroud G. Injectability of calcium phosphate pastes. *Biomaterials* 2005;26:1553–63. [PubMed: 15522757]
- [27]. Link DP, van den Dolder J, van den Beucken JJ, Wolke JG, Mikos AG, Jansen JA. Bone response and mechanical strength of rabbit femoral defects filled with injectable CaP cements containing TGF- β 1 loaded gelatin microspheres. *Biomaterials* 2008;29:675–82. [PubMed: 17996293]
- [28]. Brown, WE.; Chow, LC. A new calcium phosphate water setting cement. In: Brown, PW., editor. *Cements research progress*. American Ceramic Society; Westerville, OH: 1986. p. 352-79.
- [29]. Shindo ML, Costantino PD, Friedman CD, Chow LC. Facial skeletal augmentation using hydroxyapatite cement. *Arch Otolaryngol Head Neck Surg* 1993;119:185–90. [PubMed: 8427682]
- [30]. Friedman CD, Costantino PD, Takagi S, Chow LC. BoneSource hydroxyapatite cement: a novel biomaterial for craniofacial skeletal tissue engineering and reconstruction. *J Biomed Mater Res B* 1998;43:428–32.
- [31]. Xu HHK, Takagi S, Quinn JB, Chow LC. Fast-setting and anti-washout calcium phosphate scaffolds with high strength and controlled macropore formation rates. *J Biomed Mater Res A* 2004;68:725–34. [PubMed: 14986327]
- [32]. Muzzarelli RAA, Biagini G, Bellardini M, Simonelli L, Castaldini C, Fraatto G. Osteoconduction exerted by methylpyrrolidinone chitosan in dental surgery. *Biomaterials* 1993;14:39–43. [PubMed: 8425023]
- [33]. Xu HHK, Simon CG. Fast setting calcium phosphate-chitosan scaffold: mechanical properties and biocompatibility. *Biomaterials* 2005;26:1337–48. [PubMed: 15482821]
- [34]. Xu HHK, Quinn JB. Calcium phosphate cement containing resorbable fibers for short-term reinforcement and macroporosity. *Biomaterials* 2002;23:193–202. [PubMed: 11763861]
- [35]. American Society for Testing and Materials. *ASTM D 790-03: standard test methods for flexural properties of unreinforced and reinforced plastic and electrical insulating materials*. ASTM International; West Conshohocken, PA: 2004.
- [36]. Kim K, Dean D, Mikos AG, Fisher JP. Effect of initial cell seeding density on early osteogenic signal expression of rat bone marrow stromal cells cultured on cross-linked poly(propylene fumarate) disks. *Biomacromolecules* 2009;10:1810–7.
- [37]. Xu HHK, Weir MD, Burguera EF, Fraser AM. Injectable and macroporous calcium phosphate cement scaffold. *Biomaterials* 2006;27:4279–87. [PubMed: 16650891]

- [38]. Burguera EF, Xu HHK, Sun L. Injectable calcium phosphate cement: effects of powder-to-liquid ratio and needle size. *J Biomed Mater Res B* 2008;84:493–502.
- [39]. Moreau JL, Xu HHK. Mesenchymal stem cell proliferation and differentiation on an injectable calcium phosphate–chitosan composite scaffold. *Biomaterials* 2009;30:2675–82. [PubMed: 19187958]
- [40]. Lehr, JR.; Brown, EH.; Frazier, AW.; Smith, JP.; Thrasher, RD. Chemical engineering bulletin No. 6. Tennessee Valley Authority: 1967. Crystallographic properties of fertilizer compounds; p. 56
- [41]. Jäger M, Degistirici O, Knipper A, Fischer J, Sager M, Krauspe R. Bone healing and migration of cord blood-derived stem cells into a critical size femoral defect after xenotransplantation. *J Bone Miner Res* 2007;22:1224–33. [PubMed: 17451370]
- [42]. Benoit DSW, Nuttelman CR, Collins SD, Anseth KS. Synthesis and characterization of a fluvastatin-releasing hydrogel delivery system to modulate hMSC differentiation and function for bone regeneration. *Biomaterials* 2006;27:6102–10. [PubMed: 16860387]
- [43]. Hofmann S, Hagemuller H, Koch AM, Muller R, Vunjak-Novakovic G, Kaplan DL, et al. Control of in vitro tissue-engineered bone-like structures using human mesenchymal stem cells and porous silk scaffolds. *Biomaterials* 2007;28:1152–62. [PubMed: 17092555]
- [44]. Leach JK, Kaigler D, Wang Z, Krebsbach PH, Mooney DJ. Coating of VEGF-releasing scaffolds with bioactive glass for angiogenesis and bone regeneration. *Biomaterials* 2006;27:3249–55. [PubMed: 16490250]
- [45]. Reilly GC, Radin S, Chen AT, Ducheyne P. Differential alkaline phosphatase responses of rat and human bone marrow derived mesenchymal stem cells to 45S5 bioactive glass. *Biomaterials* 2007;28:4091–7. [PubMed: 17586040]
- [46]. Sitharaman B, Shi X, Walboomers XF, Liao H, Cuijpers V, Wilson LJ, et al. In vivo biocompatibility of ultra-short single-walled carbon nanotube/biodegradable polymer nanocomposites for bone tissue engineering. *Bone* 2008;43:362–70. [PubMed: 18541467]
- [47]. Shi X, Sitharaman B, Pham QP, Liang F, Wu K, Billups WE, et al. Fabrication of porous ultra-short single-walled carbon nanotube nanocomposite scaffolds for bone tissue engineering. *Biomaterials* 2007;28:4078–90. [PubMed: 17576009]
- [48]. Drury JL, Dennis RG, Mooney DJ. The tensile properties of alginate hydrogels. *Biomaterials* 2004;25:3187–99. [PubMed: 14980414]
- [49]. Kuo CK, Ma PX. Ionically crosslinked alginate hydrogels as scaffolds for tissue engineering: part I. Structure, gelation rate and mechanical properties. *Biomaterials* 2001;22:511–21. [PubMed: 11219714]
- [50]. Damien CJ, Parsons JR. Bone graft and bone graft substitutes: a review of current technology and applications. *J Appl Biomater* 1991;2:187–208. [PubMed: 10149083]
- [51]. O’Kelly K, Tancred D, McCormack B, Carr A. A quantitative technique for comparing synthetic porous hydroxyapatite structure and cancellous bone. *J Mater Sci Mater Med* 1996;7:207–13.
- [52]. Martin RB, Chapman MW, Holmes RE, Sartoris DJ, Shors EC, Gordon JE, et al. Effects of bone ingrowth on the strength and non-invasive assessment of a coralline hydroxyapatite material. *Biomaterials* 1989;10:481–8. [PubMed: 2804236]
- [53]. Temenoff JS, Park H, Jabbari E, Sheffield TL, LeBaron RG, Ambrose CG, et al. In vitro osteogenic differentiation of marrow stromal cells encapsulated in biodegradable hydrogels. *J Biomed Mater Res* 2004;70A:235–44.

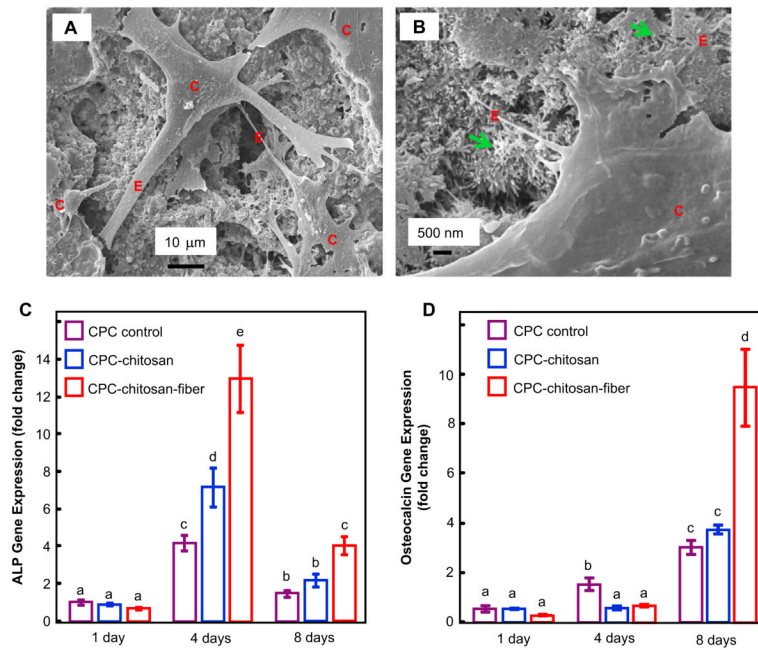


Fig. 1. hUCMSC attachment on CPC control, CPC-chitosan, and CPC-chitosan-fiber scaffolds. (A) SEM shows hUCMSCs attaching on CPC-chitosan specimen. “C” stands for hUCMSCs. “E” refers to the cytoplasmic extensions. Cells showed a healthy spreading and were similar on all materials. (B) SEM shows hUCMSCs on CPC-chitosan-fiber scaffold, with extensions anchoring to apatite nanocrystals (arrows) that make up CPC. (C) qRT-PCR for hUCMSCs yielded alkaline phosphatase (ALP) gene expression. (D) qRT-PCR yielded osteocalcin (OC) gene expression. Each value is mean \pm sd; $n = 5$. Bars with dissimilar letters indicate significantly different values ($p < 0.05$).

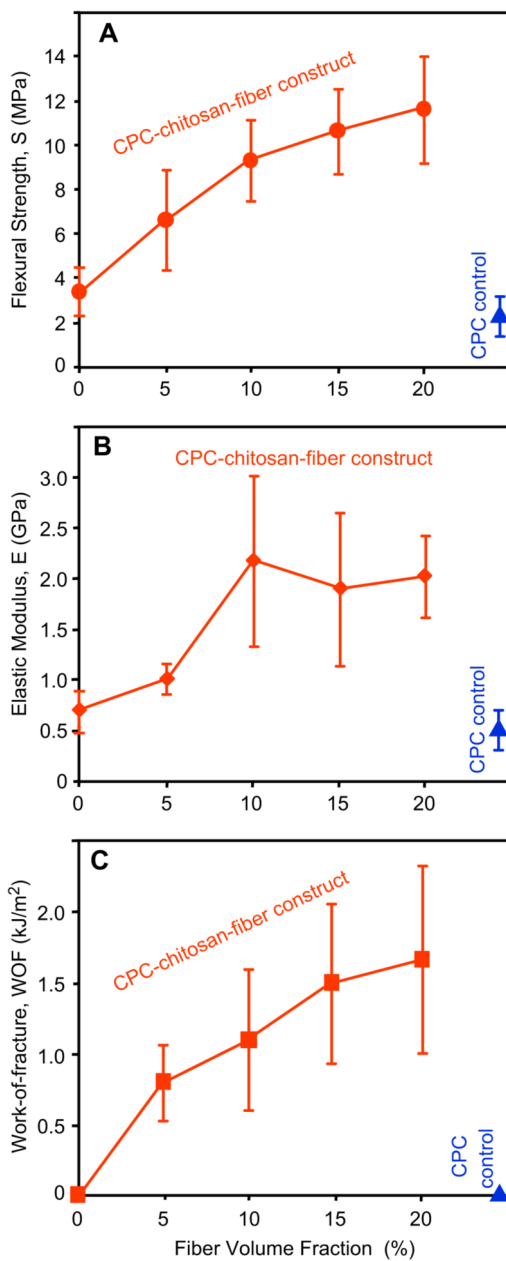


Fig. 2. hUCMSC-encapsulated CPC constructs and effect of fiber volume fraction on: (A) flexural strength, (B) elastic modulus, and (C) work-of-fracture (toughness). Each construct contained 50 vol% alginate hydrogel beads with 150,000 hUCMSCs. The CPC control with 0% chitosan and 0% fibers is included at the lower right corner. Each value is mean \pm sd; $n = 5$. Increasing the fiber volume fraction in the hUCMSC-encapsulated construct increased the mechanical properties ($p < 0.05$).

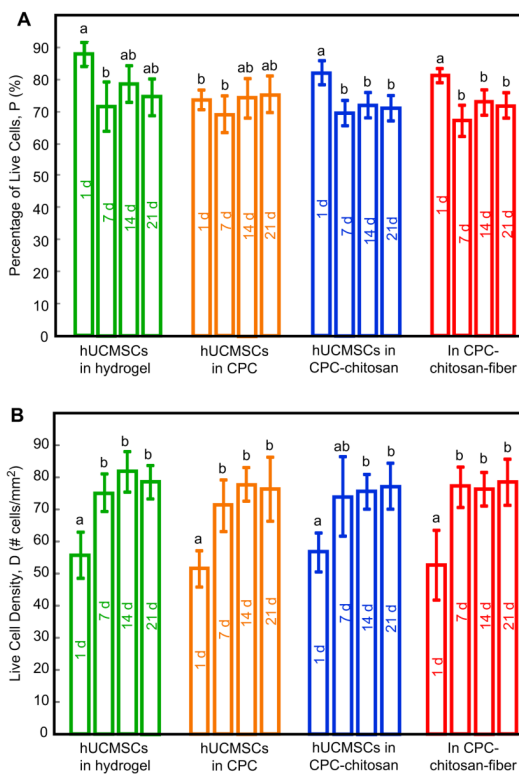
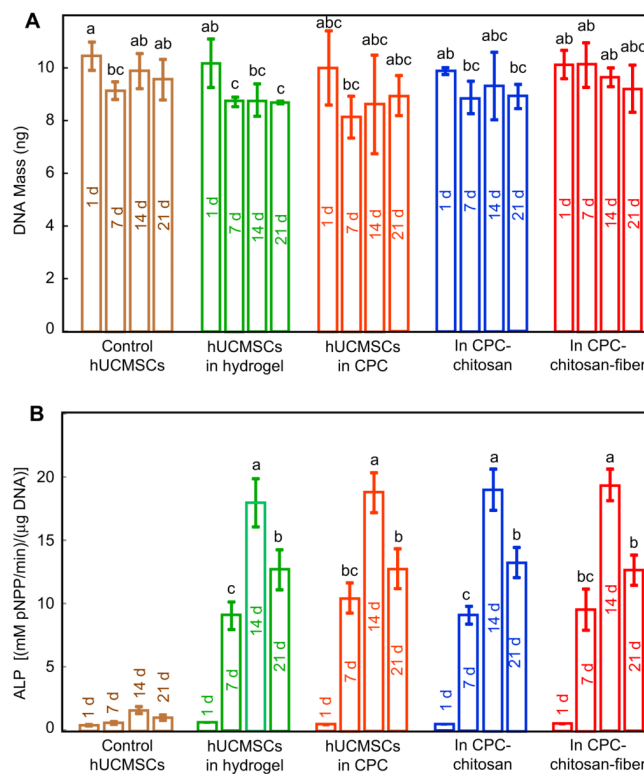


Fig. 3. hUCMSC encapsulation in constructs and cultured for 1–21 days in osteogenic media. (A) Percentage of live cells. (B) Live cell density. Each value is mean ± sd; $n = 5$. In each plot, bars with dissimilar letters indicate values that are different ($p < 0.05$). In all the constructs, hUCMSCs retained the viability and live cell density while being encapsulated for 1–21 days.

**Fig. 4.**

Osteogenic differentiation of hUCMSCs while being encapsulated in the constructs. (A) DNA content, (B) ALP, measured using a colorimetric *p*-nitrophenyl phosphate (pNPP) assay and normalized by the DNA. Each value is mean \pm sd; $n = 5$. In each plot, bars with dissimilar letters indicate values that are significantly different ($p < 0.05$). The control hUCMSCs were cultured in control media. All other constructs were cultured in osteogenic media. ALP increased substantially at 7 days, peaked at 14 days, and slightly decreased at 21 days. Chitosan, polyglactin fibers, and CPC had no adverse effects on ALP, when compared to cells in hydrogel without CPC ($p > 0.1$).

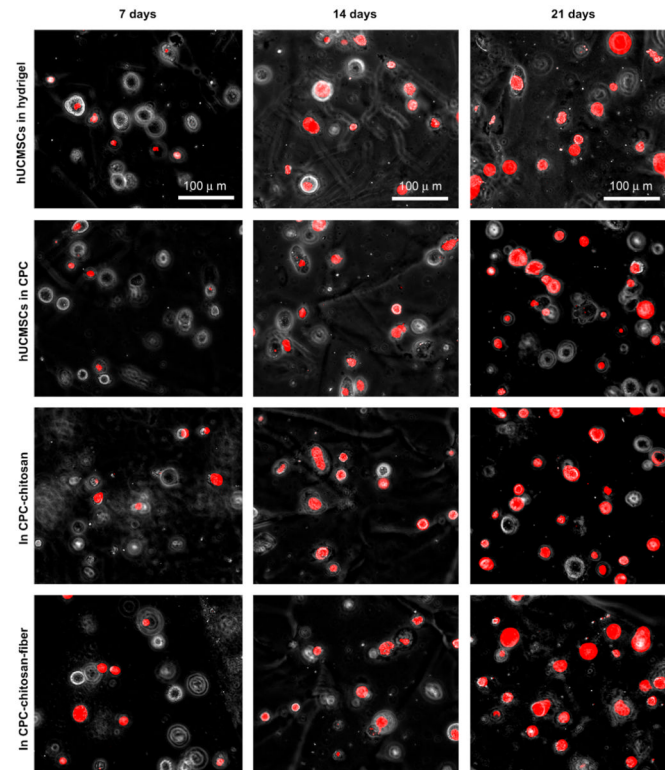


Fig. 5. hUCMSC mineralization while encapsulated in the constructs. Four constructs were tested: (1) hUCMSCs in hydrogel beads; (2) hUCMSCs in beads in CPC; (3) hUCMSCs in beads in CPC–chitosan; (4) hUCMSCs in beads in CPC–chitosan–fiber scaffold. hUCMSCs osteo-differentiated and synthesized minerals in all four constructs. Mineral content stained by xylenol orange emitted red fluorescence. Mineralization increased with time. Adding chitosan and fibers, which greatly improved the load-bearing properties, did not compromise mineralization by the hUCMSCs in CPC.

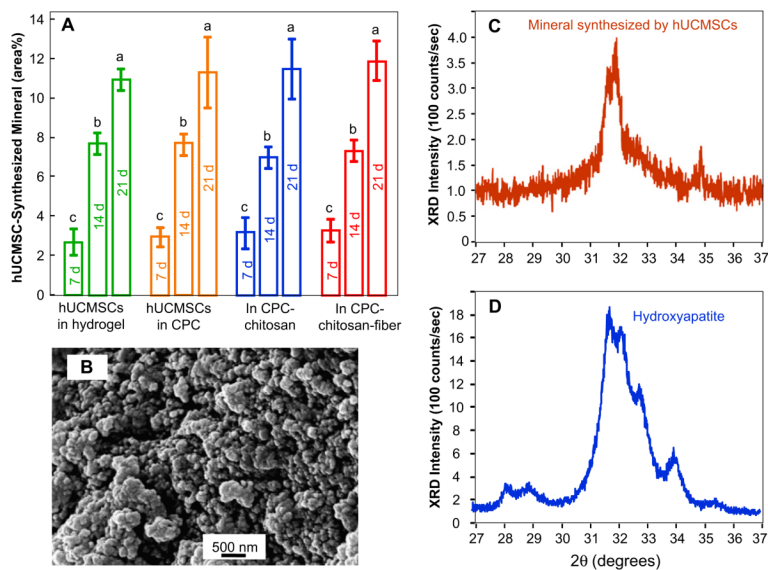


Fig. 6. Bone mineral synthesis by hUCMSCs. (A) Mineral area percentage. (B) SEM of minerals synthesized by the encapsulated hUCMSCs. (C) XRD pattern of the minerals synthesized by the hUCMSC. (D) XRD of a known hydroxyapatite formed at a physiological temperature of 37 °C, provided by Dr. Shozo Takagi at the National Institute of Standards and Technology. The XRD patterns confirm that the substance made by the cells was apatitic. The lower height of the XRD peaks for the cell-synthesized minerals suggests that they were a low-crystalline apatite.